International Journal of Pharmaceutics 511 (2016) 821–830

Contents lists available at ScienceDirect

International Journal of Pharmaceutics

journal homepage: www.elsevier.com/locate/ijpharm

A novel thermo-mechanical system enhanced transdermal delivery of hydrophilic active agents by fractional ablation

Amnon C. Sintov[a,*], Maja A. Hofmann[b]

[a] Department of Biomedical Engineering, Faculty of Engineering Sciences, Laboratory for Biopharmaceutics, E.D. Bergmann Campus, Ben Gurion University of the Negev, Be'er Sheva 84105, Israel
[b] Department of Dermatology, Venerology and Allergy, Charité-Universitätsmedizin, Charitéplatz 1, 10115 Berlin, Germany

ARTICLE INFO

Article history:
Received 22 May 2016
Received in revised form 30 June 2016
Accepted 28 July 2016
Available online 29 July 2016

Keywords:
Transdermal drug delivery
Percutaneous permeation
Fractional skin ablation
Verapamil
Diclofenac
Magnesium ascorbyl phosphate

ABSTRACT

The Tixel is a novel device based on a thermo-mechanical ablation technology that combines a sophisticated motion and a temperature control. The fractional technology is used to transfer a very precise thermal energy to the skin thereby creating an array of microchannels, accompanying by no signs of pain or inconvenience. This study aimed to evaluate the effect of the Tixel on the skin permeability of three hydrophilic molecular models: verapamil hydrochloride, diclofenac sodium, and magnesium ascorbyl phosphate. Tixel's gold-platted stainless steel tip heated to a temperature of 400 °C was applied on skin for 8 ms or 9 ms at a protrusion of 400 μm (the distance in which the tip protrudes beyond the distance gauge). The experiments were carried out partly *in vivo* in humans using a fluorescent dye and a confocal microscopy and partly *in vitro* using porcine skin and a Franz diffusion cell system. The results obtained in this study have shown that (a) no significant collateral damage to the skin tissue and no necrosis or dermal coagulation have been noted, (b) the microchannels remained open and endured for at least 6 h, and (c) the skin permeability of hydrophilic molecules, which poorly penetrate the lipophilic stratum corneum barrier, was significantly enhanced by using Tixel's pretreatment.

1. Introduction

Transdermal drug delivery has been well-established as a potentially advantageous alternative for many therapeutically active compounds to the parenteral and oral routes. The adverse effects due to fluctuations in plasma drug levels, the high portion of hepatic first-pass metabolism (or other factors leading a low bioavailability), as well as a short biological half-life have been important reasons to intensively explore ways how to circumvent the skin barrier. The highly lipophilic nature of the skin provides the main barrier for influx of drugs and environmental chemicals into the body. The lipophilic properties are related to the outermost keratinizing layer, the stratum corneum (10–20 μm thickness), which is impermeable to most therapeutically active compounds, in particular high-molecular weight, hydrophilic or charged substances. Nonetheless, the advantages of transdermal drug delivery have motivated intensive research activity for the purpose of circumventing the skin barrier with optimal solutions (Barry, 2001; Davis et al., 2002). Various methods have been studied, such as those based on chemical enhancers (Walters, 1989; Smith and Maibach, 1995; Ben-Shabat et al., 2007), or those rely on physical techniques including microneedles (Henry et al., 1998; McAllister et al., 2000), iontophoresis (Singh et al., 1999; Marro et al., 2001; Guy et al., 2001 Sintov and Brandys-Sitton, 2006), electroporation (Prausnitz et al., 1993; Riviere et al., 1995; Vanbever et al., 1994, 1996; Prausnitz, 1999; Hu et al., 2000), ultrasound (Ogra et al., 2008), as well as a diversity of thermal ablation techniques (Sintov et al., 2003; Park et al., 2008; Bachhav et al., 2010, 2013; Lee et al., 2011). Thermal ablation for transdermal drug delivery has included lasers (Bachhav et al., 2010, 2013), radiofrequency (Sintov et al., 2003), or superheated steam (Lee et al., 2011) devices. A pioneering work by Park et al. (2008) has shown, by screening a broad range of temperatures (25°–315 °C) and durations (100 ms–5 s), that skin permeability strongly depends on the temperature and less on the duration of heating so even shorter durations (i.e., on a microsecond timescale) might be sufficient. Lee et al. (2011) later developed a microdevice that ejects superheated steam during only 100 μs at the skin surface, demonstrating a selective removal of stratum corneum of cadaver skin without significant collateral damage to the inner tissue. Recently, a thermo-mechanical ablation (TMAb) technology has been proposed (Lask et al., 2012; Elman et al., 2016), demonstrating

* Corresponding author.
E-mail address: asintov@bgu.ac.il (A.C. Sintov).

http://dx.doi.org/10.1016/j.ijpharm.2016.07.070
0378-5173/

fractional skin vaporization, which was similar to CO_2 laser but more cost effective than the laser (Lee et al., 2011). A resurfacing treatment device, given the name 'Tixel' (Novoxel® GmbH, Lanshut, Germany), has been consequently developed using the TMAb technology (Fig. 1). It includes an array of tiny metallic pins (1.25 mm pyramid-shaped, 3×10^{-4} cm^2 surface area at the apex) called 'the tip' which is attached to a handpiece, equipped with a linear motor. By activating the handpiece, the linear motor rapidly advances the preheated tip to the skin surface at a predetermined 'protrusion' for a brief duration (Fig. 1B), thus creating micro-craters by vaporization of the stratum corneum.

In the present study, we have demonstrated the effect of the Tixel on the skin permeability of three hydrophilic molecular models – verapamil hydrochloride, diclofenac sodium, and magnesium ascorbyl phosphate. Verapamil hydrochloride is very soluble in water and most polar organic solvents. Due to its hydrophilic properties, it is an ideal molecular model for evaluation of drug delivery system aimed to enhance percutaneous absorption. Although verapamil was used in this study as a model drug, it has also been proved to be beneficial as a topical drug (transdermal electromotive administration of 15% gel) for Peyronie's disease. This is due to its ability to inhibit fibroblasts and to increase collagenase activity, resulting in breaking down and remodeling the excess collagen (Anderson et al., 2000; Levine et al., 2002; Greenfield et al., 2007; Tuygun et al., 2009). Apart from the advantageous use of verapamil in Peyronie's disease, microneedle-mediated transdermal verapamil delivery was also proposed as a beneficial technology for patients with hypertension, as application of stainless steel microneedles has increased transdermal delivery of verapamil hydrochloride across porcine ear skin (Kaur et al., 2014). Diclofenac salt was used as a hydrophilic model drug which is highly soluble in aqueous solutions as ionized salts and its penetration into the skin is dependent upon partitioning of the unionized form into the lipophilic keratinic layer (Kriwet and Müller-Goymann, 1995). Diclofenac is a commonly-used, highly effective non-steroidal anti-inflammatory agent (NSAID) in the management of acute conditions of inflammation and pain, musculoskeletal disorders, arthritis, and dysmenorhea. It is a non-selective cyclooxygenase inhibitor but possesses a slightly preferential cyclooxygenase-2 inhibition activity (Giuliano and Warner, 1999). Thus, although diclofenac is a relatively safe and tolerable NSAID, serious gastrointestinal adverse effects occasionally appear after oral administration. Owing to its adverse effects, its high portion of hepatic first-pass metabolism (~50%) and its short biological half-life, the topical application of diclofenac provides, therefore, a preferred alternative to the oral dosage forms. The diethylammoniun salt of diclofenac in a topical medication, known as Voltaren® Emulgel®, is particularly suitable for musculoskeletal pain and localized forms of non-articular rheumatism and inflammations of well-defined areas near the body surface (Kriwet and Müller-Goymann, 1993). The third active compound, which we examined as a model compound in combination with Tixel's pretreatment, was the magnesium salt of ascorbic acid derivative. Apart from its antioxidant activity as a free radical scavenger, ascorbic acid and its chemically-stable derivatives (e.g., ascorbyl palmitate and magnesium ascorbyl phosphate), are well-established lightening (or whitening) agents, especially used in south-east Asia as a stylish approach that fair skin is associated with beauty. Ascorbic acid derivatives react with copper ions at the tyrosinase active site resulted in reduction of dopaquinone, the precursor of melanin (Farris, 2005).

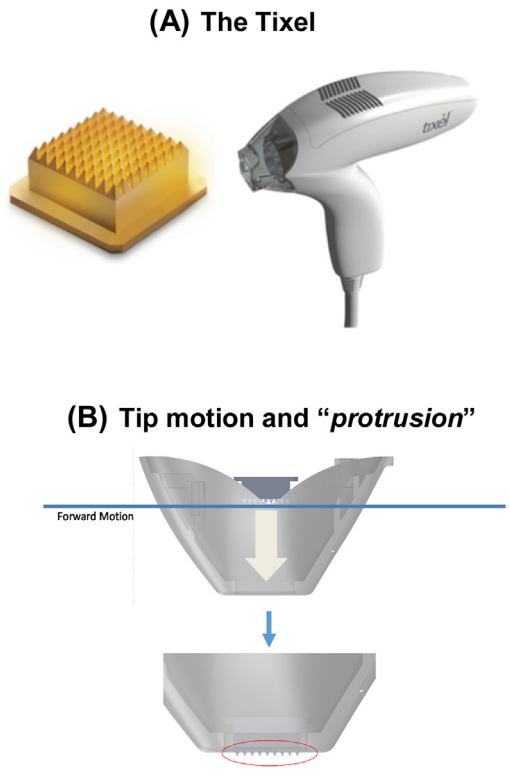

Fig. 1. The Tixel's handpiece and its metallic tip (A). Note that the term 'protrusion' refers to a distance of the pins beyond the gauge, being controlled to a desired length during tip motion operation (B).

The Tixel – TMAb technology – is presented and described in this paper. By using this device for drug delivery, we have demonstrated for the first time an increased permeability of hydrophilic active compounds. In this paper, we focus on low molecular-weight molecules as a model, which is apparently a first step in the widespread investigation of this technology. We have shown that a fractional ablation of the upper layer of the skin carried out by the Tixel's pretreatment procedure can result in an enhanced transdermal delivery of poorly permeable drugs. In addition, the microchannels or micropores formed by the Tixel-TMAb technique were microscopically observed after a histological procedure or after staining by diagnostic dyes.

2. Materials and methods

2.1. Materials

Diclofenac as a sodium salt was obtained from Sigma (Rehovot, Israel), verapamil hydrochloride was obtained from Euroasian Chemicals Pvt. Ltd. (Mumbai, India), and magnesium ascorbyl phosphate (Nikkol VC-PMG) was purchased from Nikko Chemicals (Tokyo, Japan). High-performance liquid chromatography (HPLC) grade water and organic solvents were obtained from J.T. Baker (Mallinckrodt Baker, Inc., Phillipsburg, NJ).

2.2. The Tixel

As shortly described in the Introduction section, the Tixel (Novoxel, Israel) is a thermo-mechanical system for fractional ablation, which applies a tip.

2.2.1. The Tixel's tip

The Tixel's tip is made of stainless steel (SS) plated by pure gold (Fig. 1A), being fixated at the distal section of the Tixel's handpiece. The tip's active surface consists of an array of 81 (9×9) pyramidal pins evenly spaced within a boundary area of 1×1 cm. The pin's height is 1.25 mm having a radius of about 100 μm at the apex, meaning that each miniature pyramid contacts the skin over

3×10^{-4} cm^2 surface area. The back plane of the tip is connected to a coin-size ceramic heater keeping the tip at a constant temperature of 400 °C during operation. The heater is pressed against the tip by a spring to ensure good thermal matching. When not in use, the tip is base-positioned at a distance of 2 cm from the skin's surface ('home position'). The tip is re-usable, while the system checks, validates, cleans, sterilizes and exchanges tips automatically.

2.2.2. Tip's sterility

the system is designed to sterilize the tip before the system is ready for operation. When the tip reaches the temperature of 350 °C, the system's operation is blocked until the tip is heated to temperatures varying from 350 °C to 400 °C for duration of 3 min. Tip sterility has been evaluated in accordance with the requirements of ISO 20857 (ISO 20857 Sterilization of health care products – Dry heat – Requirements for the development, validation and routine control of a sterilization process for medical devices). Sterility, which means an absence of all viable microorganisms including viruses, is measured as a probability of no more than one viable microorganism per one million sterilized items of the final product (the generally accepted pharmacopoeial sterilization procedures is called 'sterility assurance level' (or SAL) of 1×10^{-6}). Four validation tests were performed, three of these tests at a half time cycle (a sterilization cycle of 1.5 min long), and a forth test was performed at a full cycle (for 3 min). After each cycle, the tips were tested for sterility by immersing the tips inside soybean-casein digest agar medium (trypticase soy agar, TSA), resulting in a negative growth after 7-day incubation at 30 ± 1 °C. In all four tests, no growth was observed for all tested items. Following validation of the sterilization process, the theoretical ability of the Tixel system to maintain its antiseptic capability was also evaluated before and during operation, based on the different spores' lethal characteristics. The calculations were based on a statistical model from which the calculation of system sterility assurance level (SAL) had been derived (ISO 20857, 2010) (data not shown). Calculations were performed on two spore types: (a) *Bacillus atrophaeus*, and (b) *Staphylococcus aureus*, skin bacteria which commonly lead to a severe bacterial infection such as in cellulitis.

2.2.3. Tixel's operation

The handpiece weighs 270 g. When the user places the handpiece flat on the skin and activates it, the linear motor rapidly advances the tip which comes in a brief contact with the tissue. There is an opening in the distance gauge through which the tip can protrude at a desired length, perpendicular to the skin, usually 400 μm beyond the distance gauge (Fig. 1B). During tip motion the supply of electrical energy to the heater continues and all control operations are active. Controls operations include a precise monitoring of the speed, the protrusion distance and the temperature of the tip. The thermal energy is transferred to the skin, creating micropores (or micro-craters) by evaporation. The tip recedes within a precisely a controlled distance and time to its 'home position', away from the tissue. The duration of the pulse, i.e. the time of contact between the tip and the skin, can be adjusted between 6 ms to18 ms, however, we have operated the instrument at no higher than 9 ms since this time duration did not cause any coagulation or necrosis. A double pulsing mode is also enabled. The motor's displacement accuracy is in the range of 1–8 μm. Energy calculations have been previously made (Lask et al., 2012; Elman et al., 2016), showing that a 14 ms pulse duration creates a high energy of ~25 mJ/pore while a 10 ms pulse duration creates a medium energy of ~15 mJ/pore and a 6 ms pulse duration results in a low energy of ~10 mJ/pore. The utilization of the Tixel does not require any protective eyewear or a smoke evacuator.

2.3. *In-vitro* skin penetration study

Permeability of the active compounds through pig skin was determined *in vitro* with a Franz diffusion cell system (PermeGear, Inc., Hellertown, PA). The diffusion area was 1.767 cm^2 (15 mm diameter orifice), and the receptor compartment volumes was from 12 ml. The solutions in the water-jacketed cells were thermostated at 37 °C and stirred by externally driven, Teflon-coated magnetic bars. Each set of experiments was performed with at least four diffusion cells ($n \geq 4$). The use of animal skin was performed in accordance with protocols reviewed and approved by the Institutional & Use Committee, Ben Gurion University of the Negev, which complies with the Israeli Law of Human Care and Use of Laboratory Animals. Fresh pig ears were obtained from the Institute of Animal Research (Kibbutz Lahav, Israel). Full-thickness porcine skin was excised from the fresh ears of slaughtered white pigs (100 kg, aged 6 months, breeding of Landres and Large White). After subcutaneous fat was removed with a scalpel, the skin was used immediately (Sintov and Botner, 2006; Sintov and Greenberg, 2014). All skin sections were measured for transepidermal water loss (TEWL) before mounted in the diffusion cells or stored at lower temperatures until used. TEWL examinations were performed on skin pieces using Dermalab® Cortex Technology instrument, (Hadsund, Denmark) and only those pieces that the TEWL levels were less than 10 g/m^2/h were introduced for testing. The skin was placed on the receiver chambers with the stratum corneum facing upwards, and the donor chambers were then clamped in place. The excess skin was trimmed off, and the receiver chamber, defined as the side facing the dermis, was filled with phosphate buffered saline (PBS containing 10 mM PO_4^{-3}, 137 mM NaCl, and 2.7 mM KCl, pH 7.4). After 15 min of skin washing at 37 °C, the buffer was removed from the cells and the receiver chambers were refilled with fresh PBS solution. Aliquots (0.5 g each) of a solution of a test compound were applied on the skin at time = 0. Samples (2 ml) were withdrawn from the receiver solution at predetermined time intervals, and the cells were replenished up to their marked volumes with fresh buffer-ethanol solution each time. Addition of buffer solution to the receiver compartment was performed with great care to avoid trapping air beneath the dermis.

2.4. Intradermal delivery evaluation – skin extraction

In studies using magnesium ascorbyl phosphate as a model, the post-experimental skin tissue was wiped carefully with a moist cotton wool and tape-stripped (x10) to remove the residues of ascorbyl phosphate adsorbed over the stratum corneum. The tissue was then weighed and cut to small pieces and inserted into 2-ml vials. The skin pieces in each vial were extracted by 0.5 ml distilled water. The extraction was performed by incubation in a shaker (750 rpm) for 30 min. The receiver samples and the skin extracts were taken into 1.5-ml vials and kept at −20 °C until analyzed by HPLC within two days.

2.5. HPLC analysis of samples from receiver solutions and skin extracts

Aliquots of 20 μl from each vial containing verapamil, diclofenac, or ascorbyl phosphate were injected into HPLC system (Shimadzu VP series including diode-array detector for peak spectrum identification), equipped with a prepacked C_{18} column (Betasil C18, 5 μm, 250 × 4.6 mm, ThermoHypersil, UK) heated to a temperature of 30 °C.

2.5.1. Verapamil

The quantitation of verapamil was performed by integration of peaks detected at 200 nm. The samples were chromatographed using an isocratic mobile phase consisting of phosphate buffer

(0.02 M, pH 3.0)—acetonitrile (50:50) at a flow rate of 1.0 ml/min. A calibration curve (peak area versus drug concentration) was constructed by running working standard verapamil HCl solutions in PBS for every series of chromatographed samples. Calibration curves were linear over the range 0.1–100 μg/ml (0.1, 0.25, 0.5, 0.75, 1, 2.5, 5, 7.5, 10, 25, 50, 75, 100 μg/ml).

2.5.2. Diclofenac

The quantitation of diclofenac was performed by integration of peaks detected at 280 nm. The samples were chromatographed using an isocratic mobile phase consisting of acetate buffer (0.01 M, pH 6.3)—acetonitrile (60:40) at a flow rate of 1.0 ml/min. A calibration curve (peak area versus drug concentration) was constructed by running working standard sodium diclofenac solutions in PBS for every series of chromatographed samples. Calibration curves were linear over the range 0.5–75 μg/ml (0.5, 1.0, 3.0, 5.0, 7.0, 10, 20, 50, 75 μg/ml).

2.5.3. Ascorbyl phosphate

The quantitation of diclofenac was performed by integration of peaks detected at 255 nm. The samples were chromatographed using an isocratic mobile phase consisting of 75% acetate buffer (0.08 M, pH 5.0) containing 0.016% sodium edetate, 0.075% (v/v) *n*-octylamine, and 5% (v/v) methanol (Solution A) and 25% methanol (Solution B) at a flow rate of 0.9 ml/min. A calibration curve (peak area versus drug concentration) was constructed by running working standard solutions of magnesium ascorbyl phosphate (MAP) in PBS for every series of chromatographed samples. Calibration curves were linear over the range 0.1–20 μg/ml (0.1, 0.5, 1.0, 3.0, 5.0, 7.0, 10, 20 μg/ml).

2.6. Calculation of the in vitro data

A calibration curve (peak area versus drug concentration) was constructed by running standard solutions of the test compound in ethanol for each series of chromatographed samples. As a result of the sampling of large volumes from the receiver solution (and the replacement of these amounts with equal volumes of buffer), the receiver solution was constantly being diluted. Taking this process into account, the cumulative drug that permeated out into the receiver ($Q_{out}(t_n)$) at the end of the n^{th} sampling time ($n \geq 0$) was calculated according to the following equation:

$$Q_{out}(t_0) = C_{out}(t_0) = 0$$

$$Q_{out}(t) = VrC_{out}(t_n) + \sum_{i=0}^{n-1} VsC_{out}(t_n) n \geq 1$$

where $C_{out}(t_n)$ is the drug concentration in the receiver at sampling time t_n, expressed by a running number ($t = 1, 2, 3 \ldots t_n$). *Vr* and *Vs* are the constant volumes of the receiver and the sample solutions, respectively. Data was expressed as the cumulative drug permeation per unit of membrane surface area, $Q_{out}(t_n)/S$ ($S = 1.767\ cm^2$).

The steady-state fluxes (*Jss*) were calculated by linear regression interpolation of the experimental data at a steady state:

$$Jss = \Delta Q_{out}(t_n)/(\Delta t \cdot S)$$

Apparent permeability coefficients (*Kp*) were calculated according to the equation:

$$Kp = Jss/Cd$$

where *Cd* is the concentration of the test compound in the donor compartment (1.0 wt% or 1.0×10^4 μg/ml), and it assumed that under sink conditions the concentration of the test compound in the receiver compartment is negligible compared to that in the donor compartment.

2.7. Imaging of Tixel—treated skin by phenol red dyeing

Phenol red (phenolsulfonphthalein, $pK_a = 7.9$) was used to stain the channels once created. This dye is a common indicator used for monitoring pH changes. Its color gradually changes from yellow to red over the pH range 6.6–8.0. Phenol red's transition point from yellow to red occurs at pH = 7.5, which is approximately the physiological pH of body fluids. A few drops of the dye were placed on pig skin samples immediately after treated by the Tixel. After 2 h, the skin was wiped and examined under a magnifying glass.

2.8. In vivo imaging of tixel-treated skin in humans by fluorescence confocal microscopy

The experiments were carried out in 6 volunteers (healthy Caucasians aged between 33 and 61 years, female/male ratio = 1) on their lower arm skin. Institutional Helsinki Committee's approval had been granted by the local Ethics Committee (Berlin, Germany). The imaging was performed using a confocal laser scanning microscope (LSM), VivaScope 1500 multilaser (Lucid Inc, Rochester, NY, USA), which is commonly implemented for *in vivo*/*ex vivo* skin investigations. The VivaScope system allows using a laser beam in the near-infrared range (830 nm) to visualize horizontal (*en face*) sections of the human skin *in vivo* and non-invasively. Cellular details can be visualized at a high resolution and a good contrast without necessitating a biopsy and further histological processing or staining. Contrasts in the reflectance confocal microscopic (RCM) images are mainly due to variations in refractive indices of tissue structures. A near-infrared laser (785 nm, 26 mW on the skin surface) was used to analyze the skin samples in the fingerprint region (400–2000 cm^{-1}). The 785 nm excitation wavelength has been widely used for Raman measurements in the field of dermatology due to the reduced absorption and scattering by the skin and, as a result, the high penetration ability. The Raman fingerprint spectra were recorded from the skin surface down to a depth of 250 μm at increments of 10 μm. The immersion oil, the measurement window, and the skin, all possess the same refractive index of around 1.45; therefore, all the depths measured by RCM have been considered as real geometrical depth values. The acquisition time for one Raman spectrum was 5 s, and the detailed Raman profiles were acquired within the epidermis profile. A fluorescence imaging was examined in one volunteer in order to make the cellular structure visible. In this case, a fluorescent dye (0.2% fluorescein in water) was applied to the skin just before starting the LSM measurements. The stratum corneum is a penetration obstacle for sodium fluorescein, but the disruption of this horny layer by the Tixel (400 μm, 8 ms duration) enables the fluorescent probe to be used as a contrast agent for labelling the microchannels and their structures. To examine the relative sustainability of the microchannels (or microcraters), the fluorescein solution was applied 2 and 6 h after the treatment.

2.9. Histology

Skin samples were taken immediately after craters were created by the Tixel, and preserved in 4% buffered formaldehyde solution. The samples were embedded in paraffin wax, cut to a thickness of 4–5 μm, stained with hematoxylin and eosin (H&E) and examined microscopically.

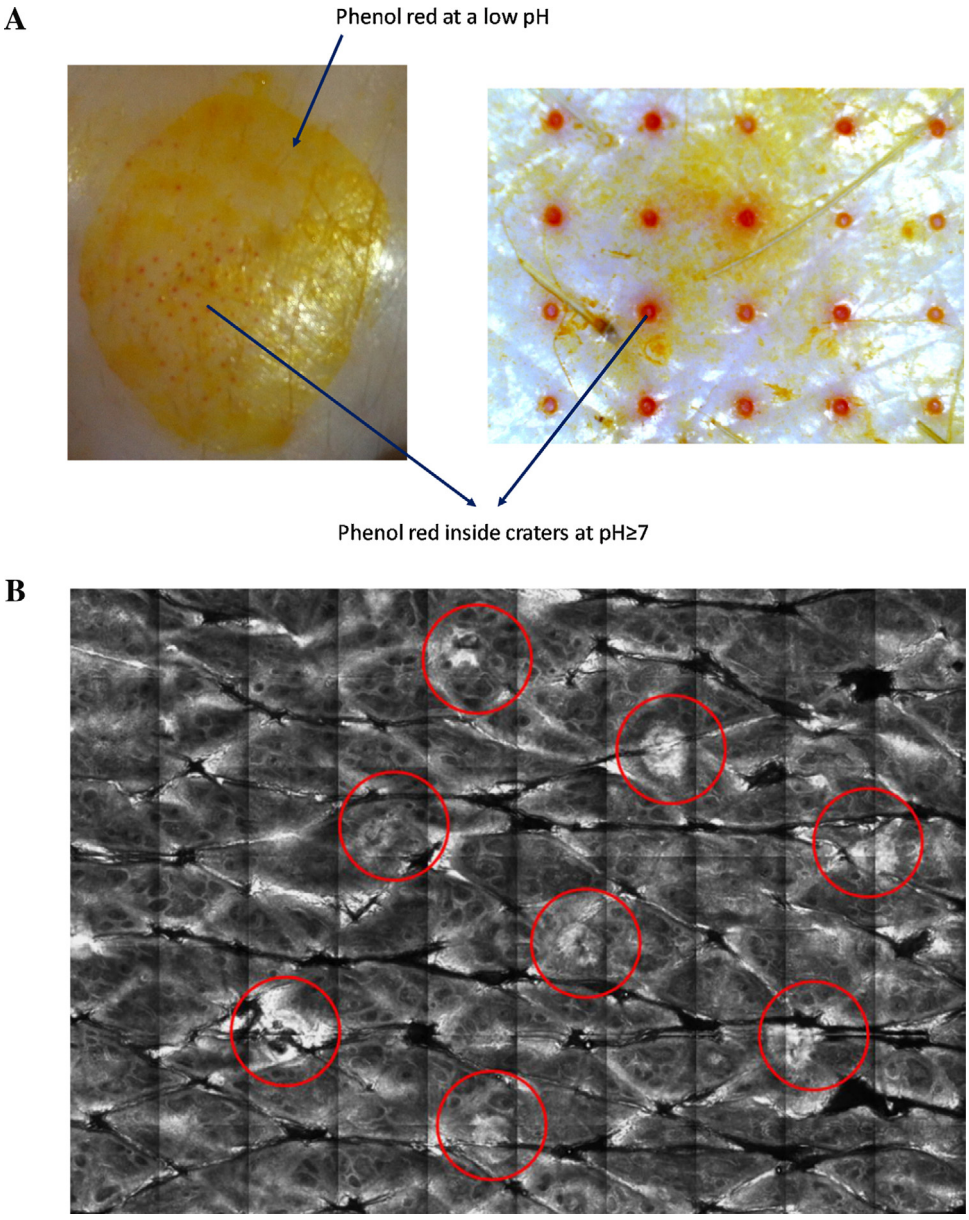

Fig. 2. A. Pig skin stained with Phenol red after Tixel treatment (400 μm protrusion, 8 ms pulse duration). Note the change from yellow to red when the dye penetrates inside the micropores, indicating an exposure to physiological pH. B. Micropores in the stratum corneum (red circles) as viewed by *in vivo* confocal microscopy on human skin (400 μm protrusion, 8 ms pulse duration). (For interpretation of the references to colour in this figure legend, the reader is referred to the web version of this article.)

3. Results and discussion

This study aimed to examine a novel thermo-mechanical technology for selective skin ablation, which does not damage the tissue or cause pain (Elman et al., 2016). The first goal was to establish by imaging and histological techniques the shape and morphology of the microchannels created through the stratum corneum by the new fractional ablative device. The penetrations of a hydrophilic fluorescent agent and a pH-sensitive dye were also imaged. The second goal was to evaluate the practical effectiveness of the method on skin permeability for the purpose of transdermal delivery of hydrophilic active agents.

3.1. Microscopic observation of Tixel-treated skin and imaging of micro-channels

After Tixel-treatment of fresh pig skin sections (8 ms, 400 μm protrusion) and dyeing with Phenol red (yellow color in the applied solution), red dots were observed (Fig. 2A) on the skin surface, most of them looked pretty much as open rings. This observation as shown in the photographs of Fig. 2A demonstrates uniform microchannels which were open enough to allow the interstitial fluid to fill them up. The fluid raised the pH to a physiological level,

Table 1
Depths (in μm) of Tixel-formed micropores as measured by confocal laser scanning microscopy.

Volunteer's code	Micropores' depth, μm		
	0 h after Tixel	2 h after Tixel	6 h after Tixel
C-L	178.19	169.30	168.17
P-S	164.57	165.78	163.56
M-L	187.45	189.01	186.73
R-S	164.59	153.54	151.20
F-K	169.17	161.75	159.73
M-H	173.74	172.41	170.56
Average (±SD)	172.95(±8.86)	168.63(±11.94)	166.65(±11.97)

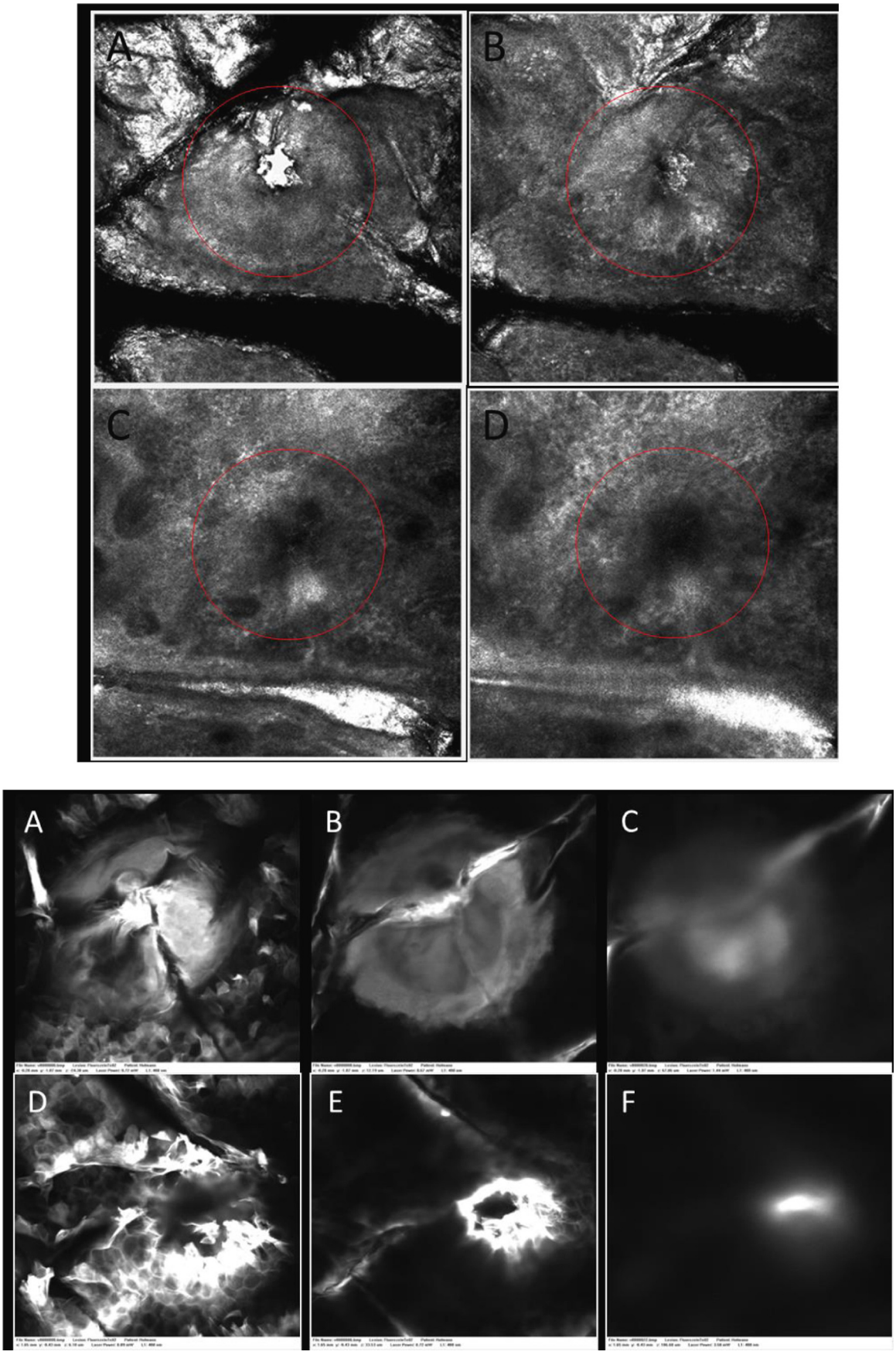

Fig. 3. Upper picture—Open microchannels generated by the Tixel as visualized *in vivo* by confocal microscope on human skin. The microchannels were stained by sodium fluorescein applied immediately after Tixel treatment. Red circle shows the microchannel (8 ms pulse): (A) skin surface, (B) epidermis layer, (C, D) papillary dermis layer. Lower

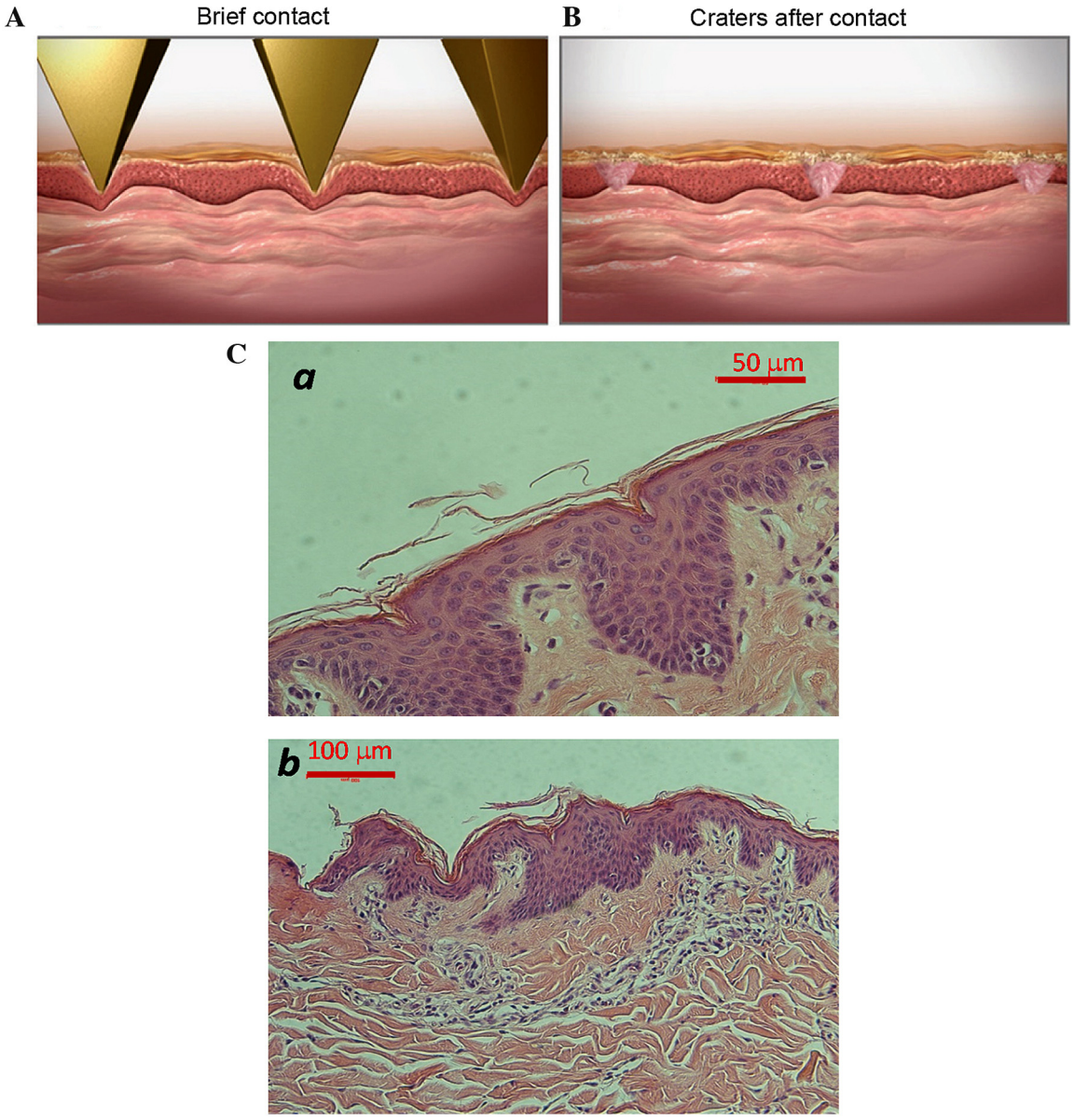

Fig. 4. Schematic presentation of the microchanneling process occurred during the high-temperature tip contact (A) and (B); Representative histological micrograph of cross-sectioned porcine skin after Tixel operation (C), 8 ms single-pulse (*a*) and 8 ms double-pulse (*b*) (400 μm protrusion).

and thereby, the dye changed its color. A fluorescent probe was also used to image penetration of hydrophilic compounds in a human volunteer after Tixel treatment. It should be noted that the *in vivo* treatment did not cause pain or inconvenience, however, very slight erythema sometimes occurred and disappeared within a few hours (Elman et al., 2016). Visualization of the microchannels by confocal microscopy showed clean holes (Fig. 2B), which remained open for at least 6 h, 172.9 ± 8.9 μm at $t = 0$, 168.6 ± 11.9 μm at $t = 2$ h, and 166.6 ± 12.0 μm at $t = 6$ h (Table 1). Fig. 3 shows that the fluorescent dye penetrated through the epidermis down to the papillary dermis *in vivo* (upper picture). Interestingly, the penetration of the fluorescent dye was enhanced when applied a few hours after Tixel treatment (Fig. 3, lower picture). The picture exemplifies the fluorescence emission in three skin layer within the epidermis, clearly demonstrating an increased intensity after 6 h compared with the intensity after 2 h post-treatment. It was evidenced therefore that (a) the microchannels endured for hours after their formation, and (b) the permeability of the hydrophilic dye even increased with time. Although the mechanism is unclear, it may imply that the ablated cells on the inside wall of the microchannel decomposed or cleared away as time has passed, enabling more permeant to undisturbedly diffuse. It is conceived that the abrupt ablation of the skin's superficial tissue is carried out by increments of thermal energy transfer during the perpendicular motion of the 400 °C-heated tip. By the first contact with the stratum corneum, water is evaporated resulting in partial cooling of the tip apex. In the next incremental movement, more surrounding cells are exposed to the advanced pin, particularly due to its pyramidal shape (Fig. 4), leading to a more water evaporation and cooling and so on until the pin retracts. Once the

picture—Diffusion of the fluorescent compound is visualized in the epidermis and the upper dermis. First row—Tixel was applied on the skin 2 h prior to the dyeing procedure, (A) 36 μm deep; (B) 54 μm deep; (C) 101 μm deep. Second row—Tixel was applied on the skin 6 h prior to imaging, (D) 30 μm deep; (E) 67 μm deep; (F) 113 μm deep. (For interpretation of the references to colour in this figure legend, the reader is referred to the web version of this article.)

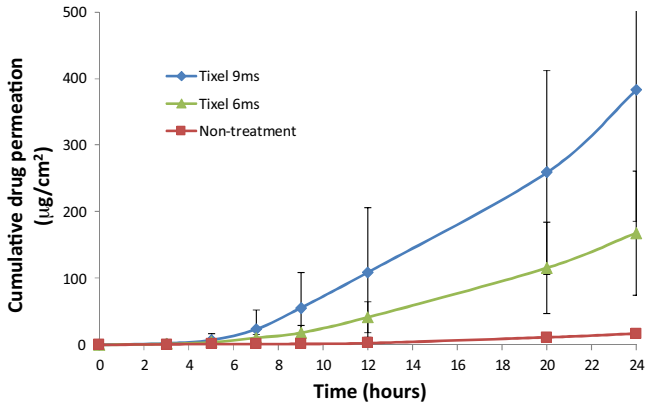

Fig. 5. Percutaneous permeation of verapamil hydrochloride (1% aqueous solution) through Tixel-pretreated pig skin at 6 ms (n = 5) and 9 ms (n = 9) pulse durations (400 μm protrusion) compared with untreated skin (n = 6). Drug permeation is expressed in μg per cm^2 of skin surface area vs. time in hours.

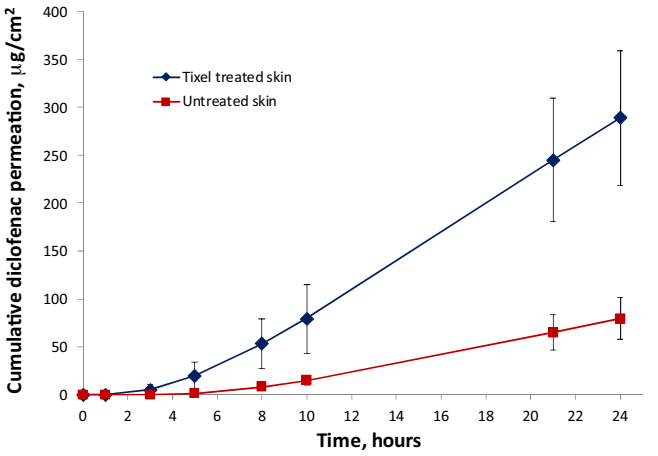

Fig. 6. Percutaneous permeation of sodium diclofenac (1% aqueous solution) through Tixel-pretreated pig skin at 8 ms pulse duration (and 400 μm protrusion) (n = 6) compared with untreated skin (n = 5). Drug permeation is expressed in μg per cm^2 of skin surface area vs. time in hours.

Tixel is activated, the very brief pulse combining with the low thermal conducting metal of the tip result in a minimal but sufficient energy for creation of water vapors. Thus, the generated water vapors carry most of the energy away sparing the viable epidermis and deeper skin tissues from a significant collateral thermal damage. Fig. 4C(*a*, *b*) shows cross-section histological micrographs of pig skin after treated by Tixel (SS tip, 400 μm protrusion; a. 8 ms single pulse, and b. 8 ms double-pulse). As observed in the micrographs, there was minimal damage to the epidermis with no necrosis or dermal coagulation.

3.2. Effect of the Tixel on skin permeability

The *in vivo* study has shown that (1) there was no real tissue damage when the Tixel had been operated in short durations (<9 ms) and a protrusion of 400 μm, (2) the diffusion of a hydrophilic dye such as fluorescein sodium confronted less impedance, due to an increase in skin permeability, and (3) the formed microchannels remained open or ajar for at least 6 h. Although application of a drug several hours after Tixel pretreatment is not clinically practical, it is an important finding suggesting that variations in the time interval from Tixel pretreatment to drug treatment would not be that critical for the therapeutic adequacy. Nonetheless, the latter *in vivo* finding is not relevant to the *in vitro* studies, in which the ablated luminal tissue of the microchannels in excised skin cannot be disintegrated and cleared to facilitate drug permeability. The *in vitro* permeation tests of drugs has been examined and determined after a single-pulse of the Tixel stainless steel tip. Although double-pulse might have resulted in a higher drug permeability (Fig. 4*b*), it was beyond the scope of this study aiming to only provide a proof of concept for the Tixel's function as an effective facilitating device for transdermal drug delivery.

3.2.1. Verapamil hydrochloride

Fig. 5 illustrates the transdermal permeation of verapamil. As shown, the penetration of verapamil hydrochloride increased about 10 and 20 times after skin had been pretreated with Tixel system for 6 ms and 9 ms, respectively ($Q_{24} = 168.2 \pm 93.0$ and 382.6 ± 196.8 μg/cm^2 compared to $Q_{24} = 17.0 \pm 6.1$ μg/cm^2 in untreated skin; $p < 0.05$, Student's *t*-test) (Table 2). In addition, lag time to get quantitative permeation across the skin decreased significantly from 9 to 10 h in untreated skin to 5 h in Tixel-treated skin. The permeability coefficient (*Kp*) of verapamil increased from 0.95×10^{-4} ($\pm 0.40 \times 10^{-4}$) cm/h in untreated skin to 9.32×10^{-4} ($\pm 5.40 \times 10^{-4}$) and 20.60×10^{-4} ($\pm 10.15 \times 10^{-4}$) cm/h in Tixel-pretreated skin at 6 ms and 9 ms pulse durations, respectively (Table 2 and Fig. 5).

3.2.2. Diclofenac sodium

Fig. 6 illustrates the transdermal permeation of the diclofenac. The penetration of sodium diclofenac increased about 3 times after skin had been pretreated with Tixel system for 8 ms ($Q_{24} = 289.1 \pm 70.5$ μg/cm^2 compared to $Q_{24} = 79.4 \pm 21.7$ μg/cm^2 in untreated skin; $p < 0.05$, Studetnt's *t*-test) (Table 2). In addition, lag time to get quantitative permeation across the skin decreased significantly from 5 h in untreated skin to 3 h in Tixel-treated skin. The permeability coefficient (*Kp*) of diclofenac increased from 4.26×10^{-4} ($\pm 1.18 \times 10^{-4}$) cm/h in untreated skin to 14.47×10^{-4} ($\pm 3.07 \times 10^{-4}$) cm/h in Tixel-pretreated skin (Table 2).

3.2.3. Magnesium ascorbyl phosphate

Fig. 7A illustrates the transdermal permeation of the ascorbyl phosphate. While no permeation was noted through untreated

Table 2
Apparent permeability coefficient (*Kp*) values of active compounds (in 1% aqueous solutions).

Active Substance	*Kp* (±SD) × 10^4 [cm/h]		Q_{end} (±SD) [μg/cm^2]	
	Non-Treatment	Tixel-treatment	Non-Treatment	Tixel-treatment
Verapamil	0.95 (±0.40)	6 ms: 9.32 (±5.40) 9 ms: 20.60 (±10.15)	17.0 (±6.1)	6 ms: 168.2 (±93.0) 9 ms: 382.6 (±196.8)
Diclofenac	4.26 (±1.18)	14.47 (±3.07) [a]	79.4 (±21.7)	289.1 (±70.5) [a]
Ascorbyl phosphate	0	2.02 (±0.49) [a]	0	10.5 (±1.8) [a]

[a] Skin was pretreated by the Tixel at a 8 ms pulse duration.

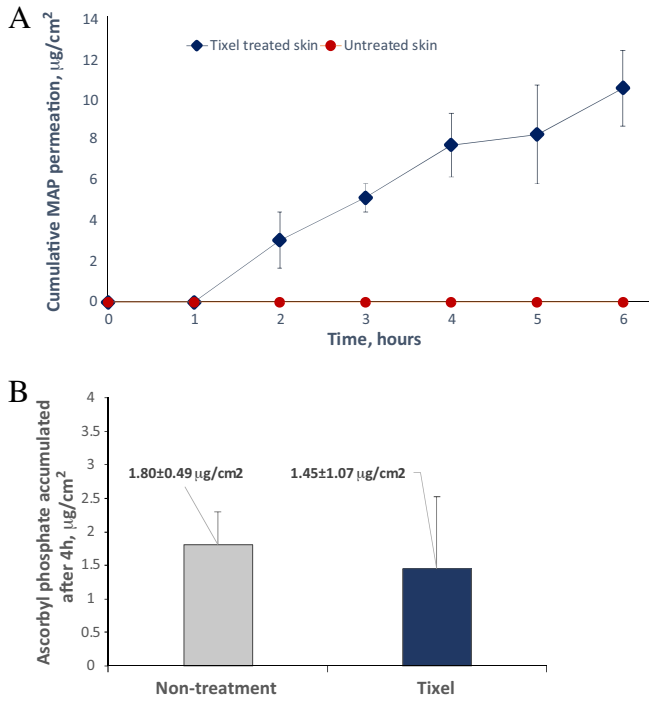

Fig. 7. Percutaneous permeation (A) and skin retention (B) of magnesium ascorbyl phosphate (1% aqueous solution) in Tixel-pretreated pig skin at 8 ms pulse duration (and 400 μm protrusion) (n = 5) compared with untreated skin (n = 5). Drug permeation is expressed in μg per cm^2 of skin surface area vs. time in hours. Drug retention is expressed in μg per cm^2 of skin surface area after 4 h.

skin, a quantitative transdermal penetration (6 h post-application) was detected after skin had been pretreated with Tixel system for 8 ms ($Q_6 = 10.5 \pm 1.8$ μg/cm^2; Table 2). The permeability coefficient (*Kp*) of the ascorbyl phosphate salt reached a value of 2.02×10^{-4} ($\pm 0.49 \times 10^{-4}$) cm/h in Tixel-pretreated skin (Table 2). Fig. 7B shows the retention of the vitamin derivative in the skin after 4 h post-application. Interestingly, no significant difference ($p > 0.05$, Student's *t*-test) has been found between the accumulative quantities within the skin although slight decrease can be denoted in the mean value determined in the Tixel-treated skin (1.45 μg/cm^2 vs. 1.80 μg/cm^2). This result has shown that the content of ascorbyl phosphate in Tixel-treated skin at steady-state was not significantly changed by the relatively high percutaneous flux created by Tixel pretreatment. However, the distribution of ascorbyl phosphate within the skin layers may be more homogeneous after Tixel pretreatment compared to untreated skin, where a high gradient of the active compound probably exists with a higher accumulation in the upper layers.

4. Conclusion

In conclusion, the results obtained in this study have shown that the skin permeability of hydrophilic molecules, which poorly penetrate the lipophilic stratum corneum barrier, was significantly enhanced by using the Tixel device. The Tixel, based on a TMAb technology, produced no skin damage in humans. The apparent safety of the fractional ablation technology is probably due to the short duration of the energy transfer, creating microchannels over a small portion of the total skin area exposed to the tip. Since the radius of each microchannel is approximately 100 μm and its surface area is 3×10^{-4} cm^2, the treated skin area is therefore occupied by only 2.4% of microchannels (the tip contains 81 pyramidal pins arrayed over a surface area of 1 cm^2). The sterility of the Tixel's tip is maintained before each operation as described in 'Materials and Methods'. After cleaning the skin by an alcohol swab, the application using a constant high temperature (400 °C) actually sterilizes the application area during the contact. After Tixel's operation, the skin might be further biosecured by utilizing aseptic or sterile topical preparations. Apart from the safety, an interesting phenomenon has been noted in the human study, which was the endurance of the microchannels hours after their formation. In addition, the permeability of the hydrophilic marker even increased with time. The mechanism of this phenomenon is not thoroughly clear and remains to be explored. The safety and the skin permeability of hydrophilic active compounds after Tixel's double-pulse (or multi-pulse) pretreatments of the skin should also be further experimented. In addition, high molecular weight compounds, such as proteins and polysaccharides, are remained to be studied widening the potential uses of the Tixel.

Acknowledgments

The authors are grateful for the professional assistance of Ms. Lillia Shapiro and Mr. Igor Greenberg at the Laboratory for Biopharmaceutics. We also gratefully acknowledge the help of the Institute of Pathology's laboratories at Soroka University Medical Center, Be'er Sheva, Israel.

References

Anderson, M.S., Shankey, T.V., Lubrano, T., Mulhall, J.P., 2000. Inhibition of Peyronie's plaque fibroblast proliferation by biologic agents. Int. J. Impot. Res. Suppl. 3, S25–31.
Bachhav, Y.G., Summer, S., Heinrich, A., Braganga, T., Bohler, C., Kalia, Y.N., 2010. Effect of controlled laser microporation on drug transport kinetics into and across the skin. J. Control. Release 146, 31–36.
Bachhav, Y.G., Heinrich, A., Kalia, Y.N., 2013. Controlled intra- and transdermal protein delivery using a minimally invasive Erbium:YAG fractional laser ablation technology. Eur. J. Pharm. Biopharm. 84, 355–364.
Barry, B.W., 2001. Novel mechanisms and devices to enable successful transdermal drug delivery. Europ. J. Pharm. Sci. 14, 101–114.
Ben-Shabat, S., Baruch, N., Sintov, A.C., 2007. Conjugates of unsaturated fatty acids with propylene glycol as potentially less-irritant skin penetration enhancers. Drug Dev. Ind. Pharm. 33, 1169–1175.
Davis, A.F., Gyurik, R.J., Hadgraft, J., Pellett, M.A., Walters, K.A., 2002. Formulation strategies for modulating skin penetration. In: Walters, K.A. (Ed.), Dermatological and Transdermal Formulations.. Marcel Dekker Inc, New York, pp. 271–317.
Elman, M., Fournier, N., Barneon, G., Hofmann, M., Bernstein, M.D., Lask, G., 2016. Fractional treatment of aging skin with tixel, a clinical and histological evaluation. J. Cosmet. Laser Ther. 20, 1–7.
Farris, P.K., 2005. Topical vitamin C: a useful agent for treating photoaging and other dermatologic conditions. Dermatol. Surg. 31, 814–817 (review).
Giuliano, F., Warner, T.D., 1999. Ex vivo assay to determine the cyclooxygenase selectivity of non-steroidal anti-inflammatory drugs. Br. J. Pharmacol. 126, 1824–1830.
Greenfield, J.M., Shah, S.J., Levine, L.A., 2007. Verapamil versus saline in electromotive drug administration for Peyronie's disease: a double-blind, placebo controlled trial. J. Urol. 177, 972–975.
Guy, R.H., Delgado-Charro, M.B., Kalia, Y.N., 2001. Iontophoretic transport across the skin. Skin Pharmacol. Appl. Skin Physiol. 14, 35–40.
Henry, S., McAllister, D.V., Allen, M.G., Prausnitz, M.R., 1998. Microfabricated microneedles: a novel approach to transdermal drug. J. Pharm. Sci. 87, 922–925.
Hu, Q., Liang, W., Bao, J., Ping, Q., 2000. Enhanced transdermal delivery of tetracaine by electroporation. Int. J. Pharm. 202, 121–124.
Kaur, M., Ita, K.B., Popova, I.E., Parikh, S.J., Bair, D.A., 2014. Microneedle-assisted delivery of verapamil hydrochloride and amlodipine besylate. Europ. J. Pharm. Biopharm. 86, 284–291.
Kriwet, K., Müller-Goymann, C.C., 1993. Binary diclofenac diethylamine-water systems, micelles, vesicles, and lyotropic liquid crystals. Eur. J. Pharm. Biopharm. 39, 234–238.
Kriwet, K., Müller-Goymann, C.C., 1995. Diclofenac release from phospholipid drug systems and permeation through excised human stratum corneum. Int. J. Pharm. 125, 231–242.
Lask, G., Elman, M., Fournier, N., Slatkine, M., 2012. Fractional vaporization of tissue with an oscillatory array of high temperature rods –Part I: ex vivo study. J. Cosmet. Laser Ther. 5, 218–223.
Lee, J.W., Gadiraju, P., Park, J.H., Allen, M.G., Praunitz, M.R., 2011. Microsecond thermal ablation of skin for transdermal drug delivery. J. Control. Release 54, 58–68.
Levine, L.A., Goldman, K.E., Greenfield, J.M., 2002. Experience with intraplaque injection of verapamil for Peyronie's Disease. J. Urol. 168, 621–626.

Marro, D., Guy, R.H., Delgado-Charro, M.B., 2001. Characterization of the iontophoretic permselectivity properties of human and pig skin. J. Control. Release 70, 213–217.
McAllister, D.V., Allen, M.G., Prausnitz, M.R., 2000. Microfabricated microneedles for gene and drug delivery. Ann. Rev. Biomed. Eng. 2, 298–313.
Ogra, M., Pahwal, S., Mitragotri, S., 2008. Low frequency sonophoresis: current status and future prospects. Adv. Drug Delivery Rev. 60, 1218–1223.
Park, J.H., Lee, J.W., Kim, Y.C., Prausnitz, M.R., 2008. The effect of heat on skin permeability. Int. J. Pharm. 359, 94–103.
Prausnitz, M.R., Bose, V.G., Langer, R., Weaver, J., 1993. 1993: Electroporation of mammalian skin: a mechanism to enhance transdermal drug delivery. Proc. Natl. Acad. Sci. U. S. A. 90, 10504–10508.
Prausnitz, M.R., 1999. A practical assessment of transdermal drug delivery by skin electroporation. Adv. Drug Delivery Rev. 35, 61–76.
Riviere, J.E., Monteiro-Riviere, N.A., Rogers, R.A., Bommannan, D., Tamada, J.A., Potts, R.O., 1995. Pulsatile transdermal delivery of LHRH using electroporation: drug delivery and skin toxicology. J. Control. Release 36, 229–233.
Singh, P., Liu, P., Dinh, S.M., 1999. Facilitated transdermal delivery by iontophoresis, In: Bronaugh, R.L., Maibach, H.I. (Eds.), Percutaneous Absorption, Drugs-Cosmetics-Mechanisms-Methodology.. 3rd ed. Marcel Dekker Inc, New York, pp. 633–657.
Sintov, A.C., Botner, S., 2006. Transdermal drug delivery using microemulsion and aqueous systems: influence of skin storage conditions on the in vitro permeability of diclofenac from aqueous vehicle systems. Int. J. Pharm. 311, 55–62.
Sintov, A.C., Brandys-Sitton, R., 2006. Facilitated skin penetration of lidocaine: combination of a short-term iontophoresis and microemulsion formulation. Int. J. Pharm. 316, 58–67.
Sintov, A.C., Greenberg, I., 2014. Comparative percutaneous permeation study using caffeine-loaded microemulsion showing low reliability of the frozen/thawed skin models. Int. J. Pharm. 471, 516–524.
Sintov, A.C., Krymberk, I., Daniel, D., Hannan, T., Sohn, Z., Levin, G., 2003. Radiofrequency–driven skin microchanneling as a new way for electrically assisted transdermal delivery of hydrophilic drugs. J. Control. Release 89, 311–320.
Smith, E.W., Maibach, H.I., 1995. Percutaneous Penetration Enhancers. CRC Press, Boca Raton, FL.
Tuygun, C., Ozok, U.H., Gucuk, A., Bozkurt, I.H., Imamoglu, M.A., 2009. The effectiveness of transdermal electromotive administration with verapamil and dexamethasone in the treatment of Peyronie's disease. Int. Urol. Nephrol. 41, 113–118.
Vanbever, R., Lecouturier, N., Preat, V., 1994. Transdermal delivery of metoprolol by electroporation. Pharm. Res. 11, 1657–1662.
Vanbever, R., Le Boulenge, E., Preat, V., 1996. Transdermal delivery of fentanyl by electroporation I. Influence of electrical factors. Pharm. Res. 13, 559–565.
Walters, K.A., 1989. Penetration enhancers and their use in transdermal therapeutic systems. In: Hadgraft, J., Guy, R.H. (Eds.), Transdermal Drug Delivery, Developmental Issues and Research Initiatives.. Marcel Dekker Inc, New York, pp. 197–246.